International Journal of Mechanical, Industrial and Aerospace Sciences
ISSN: 2517-9950
Vol:9, No:5, 2015

The Modification of the Mixed Flow Pump with Respect to Stability of the Head Curve

Roman Klas, František Pochylý, Pavel Rudolf

***Abstract*—**This paper is focused on the CFD simulation of the radiaxial pump (i.e. mixed flow pump) with the aim to detect the reasons of Y-Q characteristic instability. The main reasons of pressure pulsations were detected by means of the analysis of velocity and pressure fields within the pump combined with the theoretical approach. Consequently, the modifications of spiral case and pump suction area were made based on the knowledge of flow conditions and the shape of dissipation function. The primary design of pump geometry was created as the base model serving for the comparison of individual modification influences. The basic experimental data are available for this geometry. This approach replaced the more complicated and with respect to convergence of all computational tasks more difficult calculation for the compressible liquid flow. The modification of primary pump consisted in inserting the three fins types. Subsequently, the evaluation of pressure pulsations, specific energy curves and visualization of velocity fields were chosen as the criterion for successful design.

***Keywords*—**CFD, radiaxial pump, spiral case, stability.

I. Introduction

THE tested radiaxial pump shows the considerable pressure pulsations accompanied with the strong noise for the flow rates lower than $0.4Q_{BEP}$. This fact makes almost impossible to determine experimentally the dependence of the specific energy on the flow rates close to shut-off point. Likewise, after relatively short running period the strong wear of blades occurs due to the cavitation damage.

The above mentioned problem can be solved in two basic ways – the modification of primary hydraulic system or the complete new design. Obviously it is reasonable first to check the actual arrangement and to propose the modifications to suppress the pressure pulsations [1]. To do it, it is necessary to detect the reasons of pulsation and Y-Q characteristic instability [2]. It is shown, that it is feasible to make the analysis of the whole machine – the impeller, the spiral, the discharge throat and the suction space in view of energy dissipation. By dividing the machine into three main parts and by determination of the dissipation function curve the contribution can be estimated of the individual functional elements to the instability.

New design of any hydrodynamic pump [3]-[5] is not an easy task. The ways how to achieve it are usually well protected know-how of every specialist department. However, in many cases it is possible to use only basic relations and laws that are able to define the scope and possibilities of the new design. Some problems that can be connected with operation of hydraulic machine can be also avoided using the simple analytical and semi-empirical approaches. To the most important parameters belong the delivery head, the stability of Y-Q characteristic curves and related undesirable pressure pulsations.

Original and modified designs of radiaxial pumps with the same design parameters will be used to demonstrate the above mentioned possibilities. First the disadvantages will be outlined and then possible solutions will be illustrated. Pump operation will be simulated by means of CFD software. Experimental characteristic curve is at disposal for the problematic pump.

II. Stability Conditions

It is well known, that for the stable specific energy (head) curve (Y-Q characteristic) following condition [6] is valid in the whole range of operation

$$\frac{\partial Y}{\partial Q} < 0 \tag{1}$$

By the analysis of the pump power output and the specific energy it can be derived that the condition of the instability [7] needs to be valid for Q = 0

$$\frac{\partial^2 2D_H}{\partial Q^2} > 0 \wedge \frac{\partial 2D_H}{\partial Q} < 0 \cdot \tag{2}$$

where 2 D_H is the dissipation function depending on the flow rate. Due to problems with the exact expression of the strain rate tensor v_{ij} the balance of power inputs and outputs (3) was used as well

$$2D_H = \sum_{i=1}^{m} P_{in\,i} - \sum_{j=1}^{n} P_{out\,j} \cdot \tag{3}$$

From the experiences it is known that the unstable curve of dissipation cans generally look as in Fig. 1.

R. Klas is with the Brno University of Technology, Technická 2896/2, Brno 616 69, Czech Republic (phone: 420541142342; fax: 420541142347; e-mail: klas@fme.vutbr.cz).

F. Pochylý and P. Rudolf are with the Brno University of Technology, Technická 2896/2, Brno 616 69, Czech Republic (e-mail: pochyly@fme.vutbr.cz, rudolf@fme.vutbr.cz).

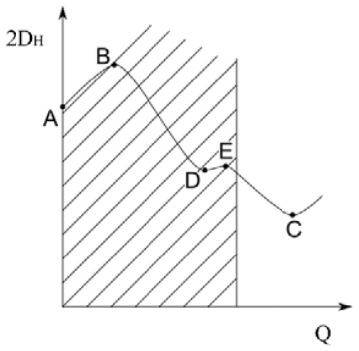

Fig. 1 Unstable curve of dissipation

III. The Primary Geometry and the CFD Simulation

The primary geometry (Pump 1) in Fig. 2 is classic radiaxial (mixed flow) pump (n_s = 330 min^{-1}) without the guide vanes [2]. The impeller is designed as open – the shroud is missing. The preprocessor GAMBIT 2.2.30. was used as the software for building of primary design including the computational mesh. For simplification the space behind the hub and also the gaps between the blades and the spiral case on the shroud side were omitted during building of the model. Predominantly hexahedral mesh contained approximately 8 millions computational cells with the worst skewness equal to 0.83.

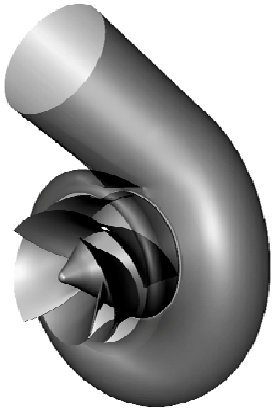

Fig. 2 The radiaxial pump, Pump 1

Consequently, the generated mesh was processed in software Ansys Fluent 12.1. The unsteady calculation of individual operating points of Y-Q characteristic was carried out with k-ε realizable turbulence model and non-equilibrium wall functions. Velocity boundary condition was used on the suction side and the pressure boundary condition on the discharge side.

IV. The Basic Approach to the Solved Problem

The correctness of the computational model was verified on the base of measured Y-Q characteristic (Figs. 11 and 15). In the next step the analysis of dissipation function in impeller, spiral and suction and discharge areas was done. Thus it was possible to estimate the share of the impeller and the spiral on the pump instability. With regard to these results the analysis of velocity and pressure fields follows. Also the proposal of preferably simple and efficient modifications of the pump geometry was made. In this context, it is suitable to use the way of dissipative function evaluation mentioned in [1].

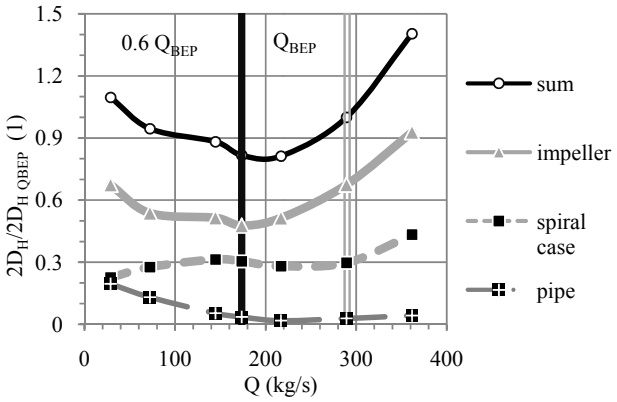

Fig. 3 Dissipated power in pump

It results from the dissipation function analysis [8], that the $2D_H$ curve in case of spiral is not optimal (Fig. 3). Therefore it is very likely that the reasons for instability have to be searched right here. Although the dependency of $2D_H$ function for impeller and also the whole curve corresponds to curves characteristic for the hydrodynamic pumps with stable specific energy curve, the magnitude of the derivative reaches relatively low values in the low flow rate region.

V. Velocity Field in the Pump Spiral Case

Fig. 4 expresses the absolute velocities field in the spiral case in the cross-sectional cut parallel to machine rotation axis for flow rates Q_{BEP} and 0.25 Q_{BEP}.

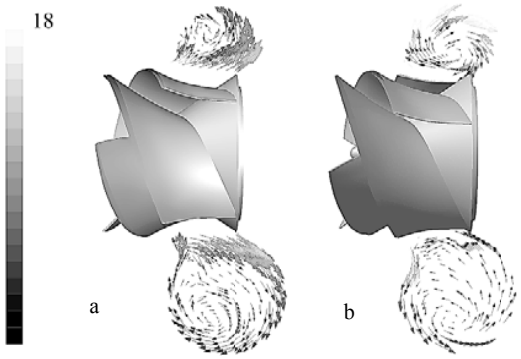

Fig. 4 Absolute velocities in the spiral, cut x =0 mm, Q_{BEP} (b) and 0.25 Q_{BEP} (a)

Illustrated velocity distribution for the mentioned flow rates represents instantaneous situation. The velocity vectors are of course changing with the impeller rotation, but Fig. 4 offers the view of the characteristic flow, that dominates in the

specific operating point of the pump.

The main character is the vortex in the spiral case. For the optimal flow rate this secondary flow occurs at the spiral case side, but the liquid is basically supplied into the spiral along the whole outlet width of the impeller (even if the velocity vectors are mainly tangential to the hub). In case of Q = 0.25 Q_{BEP} the whirl is displaced closer to the hub and the sense of its rotation is completely reversed. Then the liquid flows dominantly from the impeller along the spiral case and the outflow from the impeller is relatively low at the hub side.

VI. Modifications of Spiral Case

In the first step two modifications were applied: radial fin (Fig. 5, Fin 1) and meridional fin (Fig. 6, Fin 2). Both modifications arise from the idea to eliminate the three-dimensional vortex arising in the area behind the spiral case nose that has different sense of rotation depending on the flow rate. This vortex fills up whole flow cross-sectional area, eventually it overshoots from the hub to the opposite side (Fig. 4). This flow should be at least suppressed by inserting the first or the second fin type.

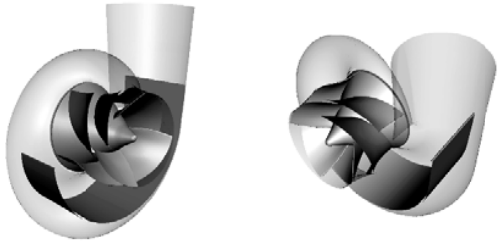

Fig. 5 Radial fin, Fin 1

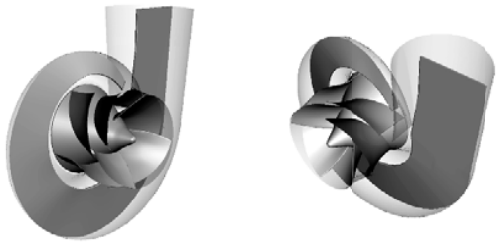

Fig. 6 Meridional fin, Fin 2

The radial fin (Fig. 5) is commonly used hydraulic component predominantly serving for decreasing the radial force that is exerted on the pump impeller. Its design and placing within the spiral case also correspond to this fact. Leading edge of the fin is defined by the plane passing the centre of the spiral case nose and by the pump shaft axis. The wrap angle of the fin is a little higher than 180° and the fin is slightly draped over to the delivery throat to entirely overlap the volute nose that does not lie in the same plane as the impeller rotation axis.

Meridional fin (Fig. 6) lies, in contrast to previous arrangement, in meridional surface. It is inserted closer to the volute nose (approximately 30° from the volute nose centre) and its trailing edge reaches the outlet area of the delivery throat. By the fin location the flow cross-sectional area of the spiral is divided into two areas with the same size. However, the complete separation of both areas immediately behind liquid outlet from the impeller does not occur. The same is also valid for the delivery throat.

VII. Monitored Parameters and Curves

As the basic criterion for the assessment of suitability of proposed modifications, Y-Q characteristic was evaluated. Also the differences of static pressures fluctuations between the pump outlet and pump inlet in dependency on the time (Figs. 7-10) or on the position of impeller were monitored. Likewise the evaluation of absolute velocities in the spiral case to observe the behaviour of the vortex and its interaction with the inserted fins was carried out. Although whole operating range was described during the analysis, the graphical representation of the results presented in this paper was reduced only to two operating points – for the optimal flow rate and close to the shut-off point.

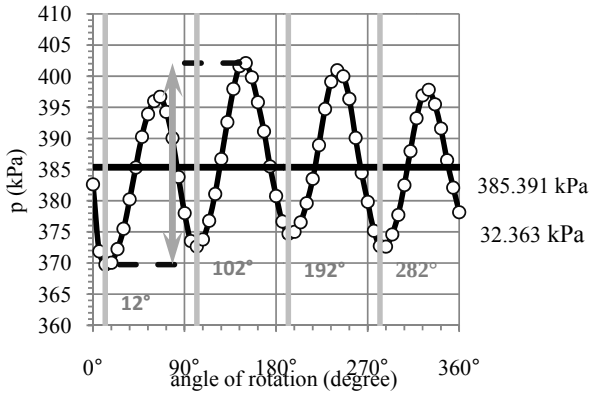

Fig. 7 Difference of the static pressures between the pump inlet and the pump outlet, Pump1, Q = 0.25 O_{BEP}

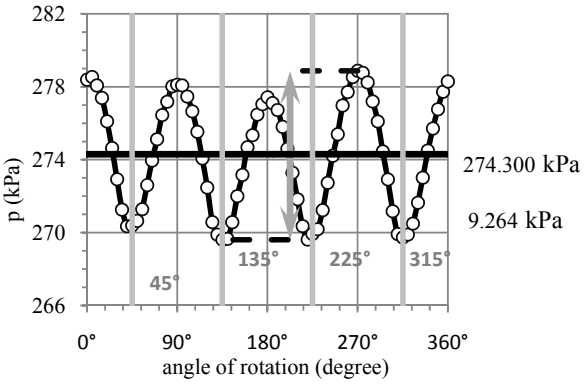

Fig. 8 Difference of the static pressures between the pump inlet and the pump outlet, Pump 1, Q = O_{BEP}

The average values of static pressures differences (Fin 1) illustrated in Fig. 9 are in comparison with Fig. 7 (Pump 1)

much lower. The same situation occurred also for the point defined as Q = 0.5 Q_{BEP}.

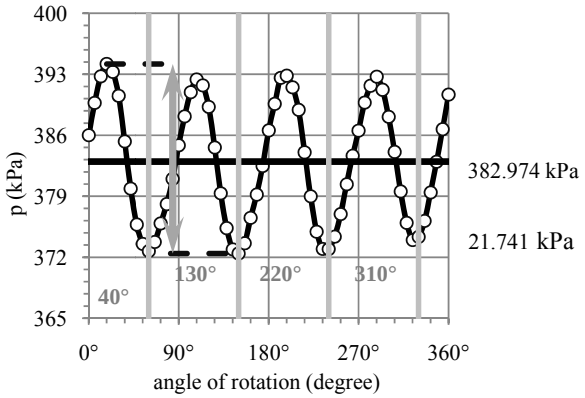

Fig. 9 Difference of the static pressures between the pump inlet and the pump outlet, Fin 1, Q = 0.25 O_{BEP}

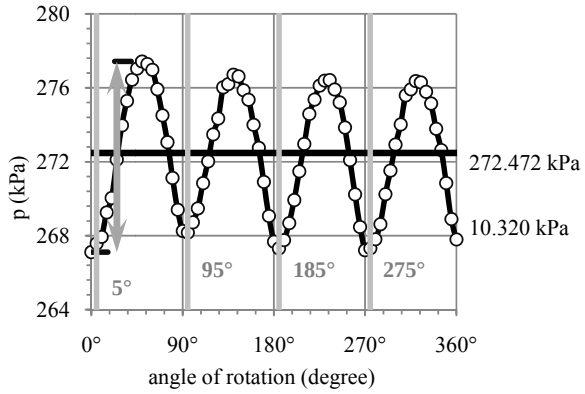

Fig. 10 Difference of the static pressures between the pump inlet and the pump outlet, Fin 1, O_{BEP}

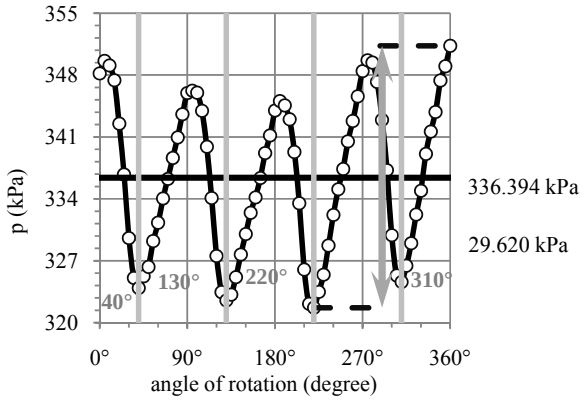

Fig. 11 Difference of the static pressures between the pump inlet and the pump outlet, Fin 2, Q = 0.25 O_{BEP}

Other modification of spiral case (Fig. 11) shows on the problems to achieve the specific energy in operation point. The reason lies in the fact, that the vortex in the spiral arose despite the inserting of the Fin 2, but it filled only the half of spiral case. So this modification relatively quickly rejected.

The evaluation of the primary design and Fin 1 will be more obvious after inspection of the graph for of specific energy (Fig. 12).

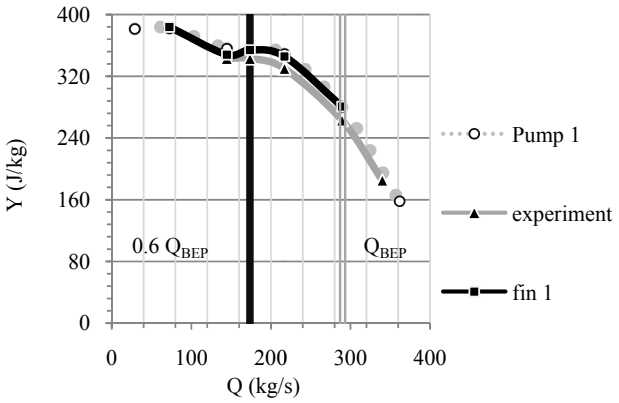

Fig. 12 Specific energy (Fin 1, Pump 1), measured characteristic curves

Fig. 12 also presents the limit of optimal flow rate and the zone where the strongest pressure pulsations occur (0.6 Q_{BEP}). From the specific energy curves and also from the static pressure curves it is obvious, that the contribution of Fin 1 is relatively small. Therefore, it can be concluded that this modification would not be suitable and effective enough.

Operating point Q = 0.1 Q_{BEP} (Pump 1) is shown in Fig. 12 too. However, regarding to the problems with the solution convergence in this area, this value of the specific energy cannot be considered to be exact and trustworthy.

VIII. The Modification of the Suction Area

Finally, after using up all design modifications for removing Y-Q curve instability, Fin 3 (Fig. 13) was inserted into the pump suction space.

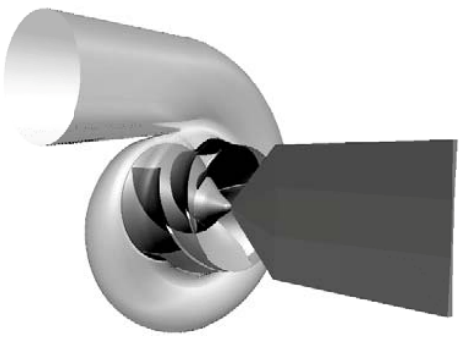

Fig. 13 Inlet area, Fin 3

This fin lies in the flow axis. This modification causes the increase of the hydraulic resistance at the pump inlet and avoids the possible liquid prerotation at the impeller inlet.

Similar to Fin 1 and Fin 2 the static pressure difference at the pump inlet and pump outlet (Figs. 14, 15) and also the Y-Q characteristic curve (Fig. 16) were evaluated. Because in this case the steady pressure difference around the average value for Q = 0.25 Q_{BEP} was not reached during the computation, the curve for pressures during rotation of the impeller is displayed (Fig. 14).

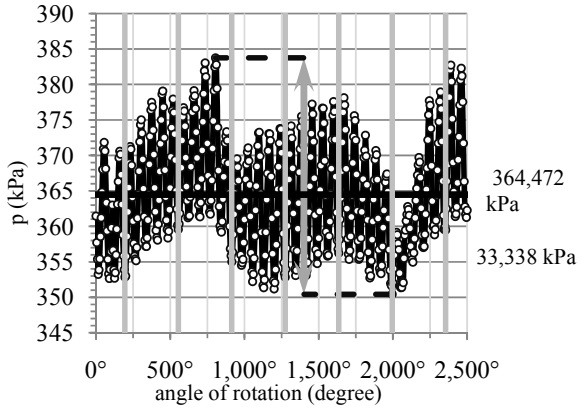

Fig. 14 Difference of the static pressures between the pump inlet and the pump outlet, Fin 3, Q = 0.25 O_{BEP}

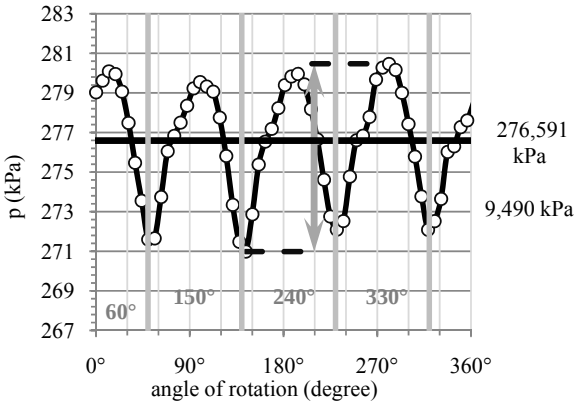

Fig. 15 Difference of the static pressure between the pump inlet and the pump outlet, Fin 3, Q = Q_{BEP}

It is obvious, that the size of pressure pulsations remained practically unchanged. The specific energy curve (Fig. 16) is slightly different, but the results are still unacceptable.

IX. Pressure and Velocity Field at the Impeller Inlet

To complete all information about the flow character inside the radiaxial pump the impeller itself was investigated too. The special attention was given to the inlet part. However, regarding to the possibilities coming from the used preprocessor GAMBIT it was not possible to create a system of planes in the impeller, which would suitably follow the meridional shape. Therefore, the relative velocities (Figs. 17, 18) and values of static pressures for pressure lower than saturation vapour pressure (Figs. 19, 20) will be displayed in the cylindrical cuts. The flow Q_{BEP} and 0.25 Q_{BEP} are monitored in the cut stretching through the centre of blade leading edge (r = 90 mm). During the flow analysis in the impeller another operating points as well as another cylindrical cuts (near the hub r = 50 mm, near the shroud r = 125 mm) were evaluated. However, neither the relative velocities curves nor the static pressure curves show different character from that presented in the following figures.

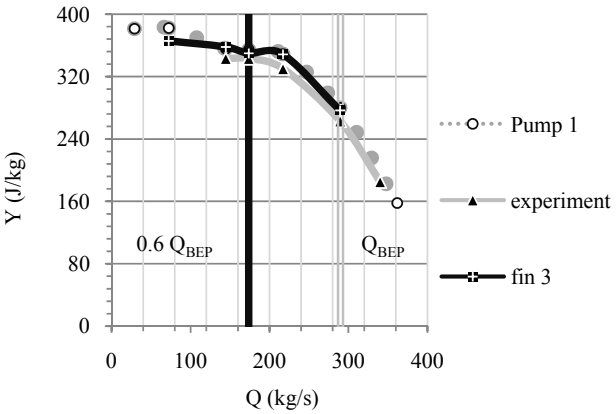

Fig. 16 Specific energy (Fin 3, Pump 1) and measured characteristic curves

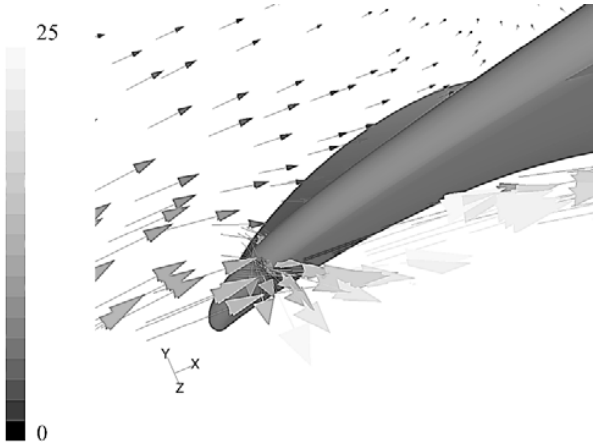

Fig. 17 Relative velocities at the blade leading edge, r = 90mm, Q = 0.25 Q_{BEP}

It is obvious, that for the flow rates near Q_{BEP} the angle of attack (the angle of relative velocity vectors) is the same as the inlet angle of blades. However, the magnitudes of the relative velocity vectors are too high. This is documented also by the pressures distribution and by the considerable risk of cavitation near the blade leading edges. Nevertheless, the cavitation can contribute to instability itself.

The scale defined in Figs. 19, 20 does not have of course any foundation from the physical point of view (one – phase CFD simulation), it only encloses the assumed cavitation area.

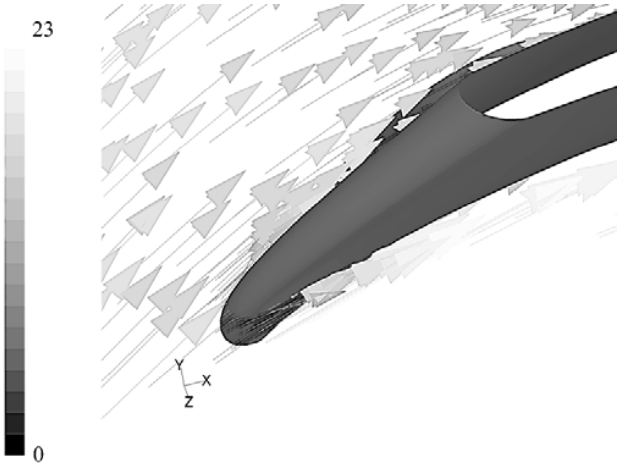

Fig. 18 Relative velocities at the blade leading edge, r = 90mm, Q = Q_{BEP}

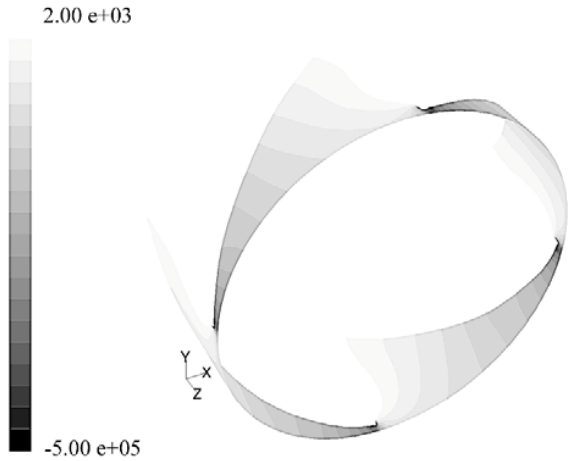

Fig. 19 Static pressures near the blade leading edge, r = 90 mm, Q = 0.25 Q_{BEP}

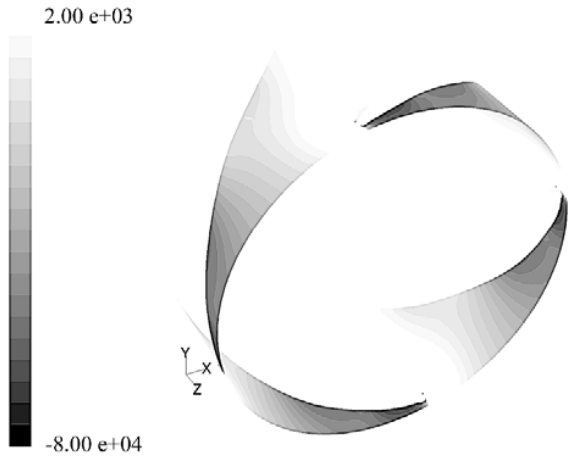

Fig. 20 Static pressures near the blade leading edge, r = 90mm, Q = Q_{BEP}

X. Conclusion

The modifications of the spiral case and the suction area of the pump did not avoid the strong pressure pulsations. Despite the effort it was not possible to prevent the undesirable secondary flows that are typical for this pump type. Because of small distance between the impeller and the spiral case nose, it is not possible to place the distributor (guide vanes) into the spiral case, which could contribute to the stabilization of the Y-Q curve.

The dissipation function seems to be very significant for evaluation of the pump performance. This function cannot provide the answer to the way how to modify the hydraulic design, but it helps in detection of the problematic functional areas. Also from the curves of this function it can be estimated the rate that the impeller, the spiral case, the inlet and outlet pipe contribute to the undesirable hydraulic losses. However the fact that the individual parts of the pump influence each other cannot be ignored.

The study of dissipation on the base of CFD analysis is described in this paper. Without this instrument we would only be able to determine the shape of dissipation function of the whole pump. Nevertheless, it is possible to obtain the idea of whole design quality. The advantage is also the simplicity of this curve, which is evaluated based on the knowledge of hydraulic efficiency and power input or power output. CFD enables to obtain dissipation also in the individual design components.

As mentioned in article, it was not possible to find an easy way for appropriate modification of the radiaxial pump primary design. However, in the beginning it was essential to properly pinpoint the reasons of instability and pressure pulsations. Therefore any instruments suitable for diagnostics of the pump behaviour are very welcome.

Acknowledgment

Project CZ.1.07/2.3.00/30.0005 “Podpora tvorby excellent ních týmů mezioborového výzkumu na VUT” is gratefully acknowledged for support of this research.

References

[1] A. Ozturk, K. Aydin, B. Sahin and A. Pinarbasi, “Effect of Impeller-Diffuser Radial Gap Ratio In a Centrifugal Pump,” in *J. Sci. Ind. Res.*, vol. 68, pp. 203–213.
[2] J. Tuzson, *Centrifugal pump design*. New York: John Wiley & Sons, 2000.
[3] D. J. Myles, “A design method for mixed flow fans and pumps,“ National Engg. Laboratory, Report No. 17, 1965.
[4] Y. Takayama, H. Watanabe, Multi-Objective Design Optimization of a Mixed flow impeller, *ASME, Summer Meeting,* Colorado, USA, 2009.
[5] M. Inoue,T. Ikui, Y. Kamada, M. Tashidaro, “A quasi three dimensional design of diagonal flow impellers by use of cascade data,“ *IAHR, 10th Symposium*, Tokyo, 1980, pp. 403–414.
[6] J. F. Gülich, *Centrifugal Pumps*. Berlin: Springer-Verlag, 2008, p.677.
[7] F. Pochylý, M. Haluza, R. Klas, “Stability of Y(Q) characteristic curve,” *IOP Conf. Ser.: Earth Environ. Sci. 12 012007*, 2010, pp. 685 – 691.
[8] F. Pochylý, M. Haluza, S. Drábková, Engineering Mechanics 2009 – book of extended abstract, 2009, pp. 208-215.